Nonlinear Modeling and Dynamic Analysis of Flexible Structures Undergoing Overall Motions Employing Mode Approximation Method

Jung-Young Kim
3rd S&D Center, Agency for Defense Development, Yuseong-Gu P. O. Box 35-3, Daejeon 305-600, Korea
Sang-Hak Hyun, Hong-Hee Yoo*
School of Mechanical Engineering, Hanyang University, Sungdong-Gu Haengdang-Dong 17, Seoul 133-791, Korea

This paper presents a nonlinear modeling method for dynamic analysis of flexible structures undergoing overall motions that employs the mode approximation method. This method, different from the naive nonlinear method that approximates only Cartesian deformation variables, approximates not only deformation variables but also strain variables. Geometric constraint relations between the strain variables and the deformation variables are introduced and incorporated into the formulation. Two numerical examples are solved and the reliability and the accuracy of the proposed formulation are examined through the numerical study.

Key Words: Flexible Structure, Nonlinear Modeling, Dynamic Analysis, Large Overall Motions, Mode Approximation Method

1. Introduction

Structures undergoing rigid body motion as well as elastic deformation can be found easily in the engineering examples such as space structures, turbine blades and memory disks. The accuracy of the dynamic analysis results for these structures is very important since lighter and more flexible structures are needed to achieve more precise and less energy spending operations these days.

For the dynamic analysis of flexible structures, several modeling methods have been introduced so far. The conventional linear modeling method (Bodley et al., 1978; Frisch, 1975; Ho, 1977) has been most widely used so far. This modeling method has several merits such as simplicity of formulation and availability of the coordinate reduction technique (Hurty et al., 1971). However, it often provides erroneous dynamic analysis results since it fails to capture proper motion-induced stiffness variation effects. To resolve this problem, several nonlinear modeling methods (Christensen and Lee, 1986; Simo and Vu-Quoc, 1986) were introduced and the accuracy problem (that the conventional linear modeling method entailed) could be remedied. However, these modeling methods have the efficiency problem due to the non-linearity and the increase of degrees of freedom.

More recently, a new linear modeling method, which is often called hybrid deformation variable modeling method, was introduced (see reference (Kane et al., 1987)). This method is as efficient as the conventional linear modeling method and as accurate as the nonlinear modeling methods introduced in the above. However, in cases when boundary conditions induce significant membrane strain, the method provides inaccurate dynamic analysis results (see reference (Yoo,

* Corresponding Author,
E-mail: hhyoo@hanyang.ac.kr
TEL: +82-2-2290-0446; **FAX**: +82-2-2293-5070
School of Mechanical Engineering, Hanyang University, Sungdong-Gu Haengdang-Dong 17, Seoul 133-791, Korea. (Manuscript **Received** September 7, 2001; **Revised** March 28, 2002)

1995)). The naive nonlinear Cartesian modeling method, introduced in Ref. Yoo (1995), could provide accurate results for the cases. However, the naive nonlinear Cartesian modeling method fails to provide accurate results when boundary conditions are not satisfied with the mode functions.

The modeling method proposed in this paper resolves the problems of the naive nonlinear Cartesian modeling method and hybrid deformation variable modeling method. The proposed method employs not only deformation variables but also strain variables to satisfy all kinds of boundary conditions. Those variables are approximated by the assumed mode method and geometric constraint relations between the strain variables and Cartesian deformation variables are incorporated into the formulation.

2. Equations of Motion

In this section, equations of motion of a rotating planar beam are derived. Figure 1 shows the configuration of the beam before and after deformation. The beam rotates about one end that is reference frame A. The other end of the beam, even though it looks free to move in this figure, may be fixed to reference frame A for different boundary conditions. The distance, between fixed end and an arbitrary point P* before deformation, is x and the deformation vector of the point is denoted as $\vec{u}$. The velocity of point P, when reference frame A rotates with angular velocity $\vec{\omega}^A$, can be obtained as

$$\vec{v}^P = \vec{v}^O + {}^A\vec{v}^P + \vec{\omega}^A \times (x\hat{a}_1 + \vec{u}) \qquad (1)$$

where $\vec{v}^O$ is the velocity of point O that is fixed

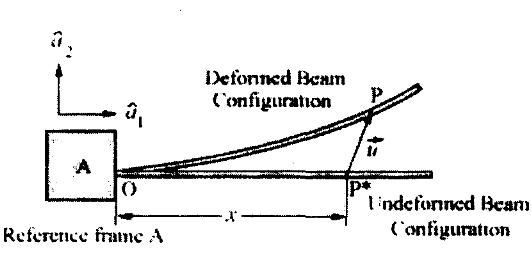

Fig. 1 Configuration of a beam before and after deformation

in the reference frame A and ${}^A\vec{v}^P$ is the relative velocity of the point P observed from the reference frame A. By using the unit vectors ($\hat{a}_1$, $\hat{a}_2$, $\hat{a}_3$) fixed to the reference frame A, each component of Eq. (1) can be expressed as follows:

$$\vec{v}^O = v_1\hat{a}_1 + v_2\hat{a}_2 \qquad (2)$$

$${}^A\vec{v}^P = \dot{u}_1\hat{a}_1 + \dot{u}_2\hat{a}_2 \qquad (3)$$

$$\vec{\omega}^A = \omega_3\hat{a}_3 \qquad (4)$$

$$\vec{u} = u_1\hat{a}_1 + u_2\hat{a}_2 \qquad (5)$$

Substituting Eqs. (2) ~ (5) into Eq. (1), Eq. (1) can be rewritten as follows:

$$\vec{v}^P = [v_1 + \dot{u}_1 - \omega_3 u_2]\hat{a}_1 + [v_2 + \dot{u}_2 + \omega_3(x + u_1)]\hat{a}_2 \qquad (6)$$

By using the velocity expression, the kinetic energy of the beam (neglecting rotary inertia effect) can be expressed as follows:

$$T = \frac{1}{2}\int_0^L \rho(\vec{v}^P)^2 dx \qquad (7)$$

where ρ represents the mass per unit area of the beam and L is the length of the beam. Also, assuming that shear and torsion are neglected, the strain energy of the beam is expressed as follows:

$$V = \frac{1}{2}\int_0^L EA\varepsilon_{11}^2 dx + \frac{1}{2}\int_0^L EI\kappa_3^2 dx \qquad (8)$$

Where E denotes Young's modulus, A is the cross-sectional area of the beam, I represents the second area moments of the cross-section, and ε_{11} and κ_3 represent the extensional strain and the curvature at point P on the elastic axis of the beam. Here, Von Karman strain is used for ε_{11}. The bending non-linearity, however, is not considered in this work. Thus, ε_{11} and κ_3 are expressed as follows:

$$\varepsilon_{11} = u_{1,x} + \frac{1}{2}(u_{2,x})^2 \qquad (9)$$

$$\kappa_3 = u_{2,xx} \qquad (10)$$

where $(\ )_{,x}$ represents the partial derivatives of $(\ )$ with respect to x.

In the present study, Cartesian variables (u_1, u_2) are employed to express the elastic deformation vector. Conventionally, the two Cartesian deformation variables are approximated to obtain ordinary differential equations of motion. In the proposed method, however, not only u_1 and u_2

but also ε_{11} and κ_3 are approximated by employing the mode approximation method as follows:

$$u_1 = \sum_{i=1}^{\mu_1} \phi_{1i} q_{1i} \tag{11}$$

$$u_2 = \sum_{i=1}^{\mu_2} \phi_{2i} q_{2i} \tag{12}$$

$$\varepsilon_{11} = \sum_{i=1}^{\nu_1} \psi_{1i} p_{1i} \tag{13}$$

$$\kappa_3 = \sum_{i=1}^{\nu_2} \psi_{2i} p_{2i} \tag{14}$$

where ϕ_{1i}, ϕ_{2i}, ψ_{1i}, and ψ_{2i} are mode functions, q_{1i}, q_{2i}, p_{1i}, and p_{2i} are their corresponding coordinates, μ_1, μ_2, ν_1, and ν_2 denote the numbers of the coordinates for u_1, u_2, ε_{11}, and κ_3, respectively. In this study, ϕ_{1i} and ϕ_{2i} are chosen from the stretching and the bending modes of the beam and ψ_{1i} and ψ_{2i} are the first derivatives of the stretching modes and the second derivatives of the bending modes.

Substituting Eqs. (11) ~ (14) into Eqs. (7) and (8), the kinetic energy and the strain energy are expressed as follows:

$$\begin{aligned} T = \frac{1}{2}\int_0^L \rho\Bigg[&\Big(v_1 + \sum_{i=1}^{\mu_1}\phi_{1i}\dot{q}_{1i} - \omega_3\sum_{i=1}^{\mu_2}\phi_{2i}q_{2i}\Big)^2 \\ &+\Big(v_2 + \sum_{i=1}^{\mu_2}\phi_{2i}\dot{q}_{2i} + \omega_3\Big(x + \sum_{i=1}^{\mu_1}\phi_{1i}q_{1i}\Big)\Big)^2\Bigg]dx \end{aligned} \tag{15}$$

$$V = \frac{1}{2}\int_0^L EA\Big(\sum_{i=1}^{\nu_1}\psi_{1i}p_{1i}\Big)^2 dx + \frac{1}{2}\int_0^L EI\Big(\sum_{i=1}^{\nu_2}\psi_{2i}p_{2i}\Big)^2 dx \tag{16}$$

Similarly, Eqs. (9) and (10) are expressed as follows:

$$\sum_{i=1}^{\nu_1}\psi_{1i}p_{1i} = \sum_{i=1}^{\mu_1}\phi_{1i,x}q_{1i} + \sum_{i=1}^{\mu_2}\frac{1}{2}\Big(\sum_i \phi_{2i,x}q_{2i}\Big)^2 \tag{17}$$

$$\sum_{i=1}^{\nu_2}\psi_{2i}p_{2i} = \sum_{i=1}^{\mu_2}\phi_{2i,xx}q_{2i} \tag{18}$$

Eqnations (15) and (16) show that kinetic energy is the function of q_{1i}, q_{2i}, $\dot{q}_{1i}$, $\dot{q}_{21}$ and the strain energy is the function of p_{1i} and p_{2i} which are additionally introduced to approximate ε_{11} and κ_3. By using Hamilton principle (see, Ref. Goldstein (1980)), the following equations of motion can be obtained.

$$\frac{\partial T}{\partial q_{1i}} - \frac{d}{dt}\Big(\frac{\partial T}{\partial \dot{q}_{1i}}\Big) - \sum_{k=1}^{\nu_1}\frac{\partial V}{\partial p_{1k}}\frac{\partial p_{1k}}{\partial q_{1i}} - \sum_{k=1}^{\nu_2}\frac{\partial V}{\partial p_{2k}}\frac{\partial p_{2k}}{\partial q_{1i}} = 0 \tag{19}$$

$$\frac{\partial T}{\partial q_{2i}} - \frac{d}{dt}\Big(\frac{\partial T}{\partial \dot{q}_{2i}}\Big) - \sum_{k=1}^{\nu_1}\frac{\partial V}{\partial p_{1k}}\frac{\partial p_{1k}}{\partial q_{2i}} - \sum_{k=1}^{\nu_2}\frac{\partial V}{\partial p_{2k}}\frac{\partial p_{2k}}{\partial q_{2i}} = 0 \tag{20}$$

As shown in Eqs. (19) ~ (20), since the coordinates p_{1i} and p_{2i} are irrelevant to the kinetic energy, terms associated with the kinetic energy are identical to those of the naive nonlinear Cartesian modeling method. The procedure to obtain the terms associated with the kinetic energy is straightforward and well explained in Ref. Yoo (1995). So, only the procedure to obtain terms associated with the strain energy will be explained here. First, the partial derivatives of the strain energy with respect to p_{1k} and p_{2k} are expressed as follows:

$$\frac{\partial V}{\partial p_{1k}} = \sum_{j=1}^{\nu_1}\int_0^L EA\psi_{1j}\psi_{1k}dx\,p_{1j} \tag{21}$$

$$\frac{\partial V}{\partial p_{2k}} = \sum_{j=1}^{\nu_2}\int_0^L EI\psi_{2j}\psi_{2k}dx\,p_{2j} \tag{22}$$

Equations (21) and (22) are expressed as the function of mode coordinates (p_{1k}, p_{2k}). These equations can be rewritten as the function of generalized coordinates (q_{1i}, q_{2i}) by using Eqs. (17) ~ (18). Multiplying Eq. (17) and Eq. (18) by $EA\psi_{1k}$ and $EI\psi_{2k}$ respectively and integrating with respect to x,

$$\begin{aligned} &\sum_{j=1}^{\nu_1}\int_0^L EA\psi_{1k}\psi_{1j}dx\,p_{1j} \\ &= \sum_{j=1}^{\mu_1}\int_0^L EA\psi_{1k}\phi_{1j,x}dx\,q_{1j} \\ &\quad + \frac{1}{2}\sum_{j=1}^{\mu_2}\sum_{m=1}^{\mu_2}\int_0^L EA\psi_{1k}\phi_{2j,x}\phi_{2m,x}dx\,q_{2j}q_{2m} \end{aligned} \tag{23}$$

$$\begin{aligned} &\sum_{j=1}^{\nu_2}\int_0^L EI\psi_{2k}\psi_{2j}dx\,p_{2j} \\ &= \sum_{j=1}^{\mu_2}\int_0^L EI\psi_{2k}\phi_{2j,xx}dx\,q_{2j} \end{aligned} \tag{24}$$

Thus, Eqs. (21)~ (22) can be rewritten as follows:

$$\begin{aligned} \frac{\partial V}{\partial p_{1k}} &= \sum_{j=1}^{\mu_1}\int_0^L EA\psi_{1k}\phi_{1j,x}dx\,q_{1j} \\ &\quad + \frac{1}{2}\sum_{j=1}^{\mu_2}\sum_{m=1}^{\mu_2}\int_0^L EA\psi_{1k}\phi_{2j,x}\phi_{2m,x}dx\,q_{2j}q_{2m} \end{aligned} \tag{25}$$

$$\frac{\partial V}{\partial p_{2k}} = \sum_{j=1}^{\mu_2}\int_0^L EI\psi_{2k}\phi_{2j,xx}dx\,q_{2j} \tag{26}$$

Employing Eqs. (25) ~ (26), Eqs. (19) and (20) will provide the equations of motion as follows:

$$\begin{aligned} &(\dot{v}_1 - \omega_3 v_2)R_{1i} - \omega_3^2 S_{1i} + \sum_{j=1}^{\mu_1} m_{ij}^{11}\ddot{q}_{1j} - \dot{\omega}_3\sum_{j=1}^{\mu_2} m_{ij}^{12}q_{2j} \\ &\quad - 2\omega_3\sum_{j=1}^{\mu_2} m_{ij}^{12}\dot{q}_{2j} - \omega_3^2\sum_{j=1}^{\mu_1} m_{ij}^{11}q_{1j} \\ &\quad + \sum_{k=1}^{\mu_1}\Big(\sum_{j=1}^{\mu_1} A_{kj}^{11}q_{1j} + \frac{1}{2}\sum_{j=1}^{\mu_2}\sum_{m=1}^{\mu_2} A_{kjm}^{122}q_{2j}q_{2m}\Big)\cdot C_{ki}^{11} = 0 \\ &\qquad\qquad (i = 1, 2, 3, \cdots, \mu_1) \end{aligned} \tag{27}$$

$$(\dot{\nu}_2+\omega_3\nu_1)R_{2i}-\dot{\omega}_3S_{2i}+\sum_{j=1}^{\mu_2}m_{ij}^{22}\ddot{q}_{2j}-\dot{\omega}_3\sum_{j=1}^{\mu_1}m_{ij}^{21}q_{1j}$$
$$+2\omega_3\sum_{j=1}^{\mu_1}m_{ij}^{21}\dot{q}_{1j}-\omega_3^2\sum_{j=1}^{\mu_2}m_{ij}^{22}q_{2j}$$
$$+\sum_{k=1}^{\mu_2}\left(\sum_{j=1}^{\mu_2}A_{kj}^{22}q_{2j}\right)\cdot C_{ki}^{22} \quad (28)$$
$$+\sum_{k=1}^{\mu_1}\left(\sum_{j=1}^{\mu_1}A_{kj}^{11}q_{1j}+\frac{1}{2}\sum_{j=1}^{\mu_2}\sum_{m=1}^{\mu_2}A_{kjm}^{122}q_{2j}q_{2m}\right)\cdot C_{ki}^{12}=0$$
$$(i=1,\ 2,\ 3,\ \cdots,\ \mu_2)$$

where,

$$R_{ai}\equiv\int_0^L\rho\phi_{ai}dx \quad (29)$$
$$S_{ai}\equiv\int_0^L\rho x\phi_{ai}dx \quad (30)$$
$$m_{ij}^{\alpha\beta}\equiv\int_0^L\rho\phi_{\alpha i}\phi_{\beta j}dx \quad (31)$$
$$A_{ij}^{11}\equiv\int_0^L EA\psi_{1i}\phi_{1j,x}dx \quad (32)$$
$$A_{ij}^{22}\equiv\int_0^L EI\psi_{2i}\phi_{2j,xx}dx \quad (33)$$
$$A_{ijk}^{122}\equiv\int_0^L EA\psi_{1i}\phi_{2j,x}\phi_{2k,x}dx \quad (34)$$
$$C_{ij}^{\alpha\beta}=\frac{\partial\phi_{\alpha i}}{\partial q_{\beta j}} \quad (35)$$

Here, $C_{ij}^{\alpha\beta}$ can be obtained from the following equations which are the partial derivatives of Eqs. (23) and (24) with respect to q_{1i} and q_{2i} respectively.

$$\sum_{k=1}^{\nu_1}K_{jk}^S\cdot C_{ki}^{11}=A_{ji}^{11} \quad (36)$$
$$\sum_{k=1}^{\nu_1}K_{jk}^S\cdot C_{ki}^{12}=\sum_{m=1}^{\mu_2}A_{jmi}^{122}q_{2m} \quad (37)$$
$$\sum_{k=1}^{\nu_2}K_{jk}^B\cdot C_{ki}^{21}=0 \quad (38)$$
$$\sum_{k=1}^{\nu_2}K_{jk}^B\cdot C_{ki}^{22}=A_{ji}^{22} \quad (39)$$

where,

$$K_{ij}^S\equiv\int_0^L EA\psi_{1i}\psi_{1j}dx \quad (40)$$
$$K_{ij}^B\equiv\int_0^L EI\psi_{2i}\psi_{2j}dx \quad (41)$$

3. Numerical Results

In this section, by using equations of motion derived in the previous section, numerical examples are solved and the results are compared with those of other modeling methods. The first example, shown in Fig. 2, is the cantilever beam attached to a rigid base that undergoes a planar rotational motion. This rotational motion is often called the spin-up motion that is given as follows:

$$\omega_3=\begin{cases}\dfrac{\Omega_S}{T_S}\left[t-\left(\dfrac{T_S}{2\pi}\right)\sin\left(\dfrac{2\pi t}{T_S}\right)\right] & \text{if } 0\le t\le T_S\\ \Omega_S & \text{if } t\ge T_S\end{cases} \quad (42)$$

where Ω_S denotes the steady state angular velocity, T_S denotes the time to reach the steady state angular velocity, and t denotes time. Numerical values used for this example are given in Table 1. Here, ϕ_{1i} and ϕ_{2i} respectively represent the stretching and the bending modes of the beam; and ψ_{1i} and ψ_{2i} respectively represent the first derivative of the stretching mode and the second derivative of the bending mode.

Table 1 Numerical data used for the simulation

Notations	Description	Numerical data
ρ	Mass per unit length of beam	1.2kg/m
E	Young's modulus of beam	7.0E10
A	Cross section area of beam	4.0E-4m^2
I	Second area moment of inertia of beam	2.0E-7m^4
L	Length of beam	10m
Ω_s	Steady state angular velocity	6rad/sec
T_s	Time to reach the steady state angular velocity	15sec

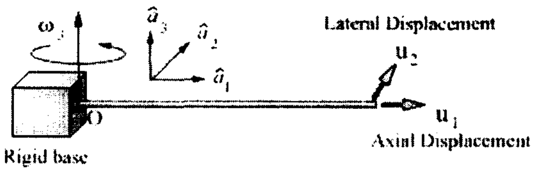

Fig. 2 Configuration of a rotating cantilever beam

Figure 3 shows the lateral displacement at the free end of the cantilever beam. Here the simulation results obtained by the proposed modeling method are drawn by the solid line, those obtained by the NNC (naive nonlinear Cartesian) modeling method are drawn by the broken solid line, and those obtained by the HDV

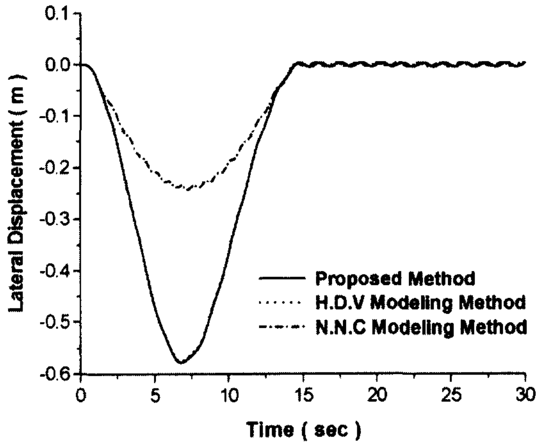

Fig. 3 Comparison of lateral displacements of cantilever beam at free end

(hybrid deformation variable) modeling method are drawn by the dotted line. For this problem, the natural boundary conditions introduced by the NNC modeling method cannot be satisfied no matter what mode functions are employed. As shown in the Fig. 3, the NNC modeling method provides incorrect results that are often named as membrane locking phenomena. The simulation results obtained by the proposed modeling method are almost identical to those obtained by the HDV modeling method. In this case, the accuracy of the HDV modeling method was verified in Ref. Yoo (1992).

Another numerical example, shown in Fig. 4, is the simply supported beam attached to rigid base that undergoes a planar rotational motion with angular velocity given in Eq. (42). Here the length of the beam is 20m, other numerical values used for the simulation are identical to the first example.

Figure 5 shows the lateral displacement at the middle point of the beam. Unlike cantilever beam, simply supported boundary condition usually induces significant membrane strain if the lateral displacement is larger than the thickness of the beam. The figure shows that the HDV modeling method fails to capture the membrane strain properly and results in incorrect solutions. On the other hand, the results obtained by the proposed modeling method are almost identical to those

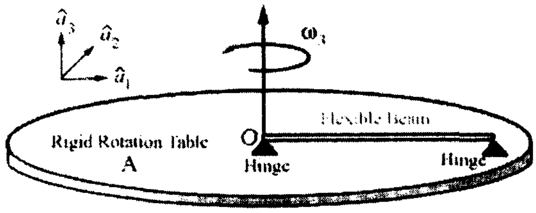

Fig. 4 Configuration of a simply supported beam

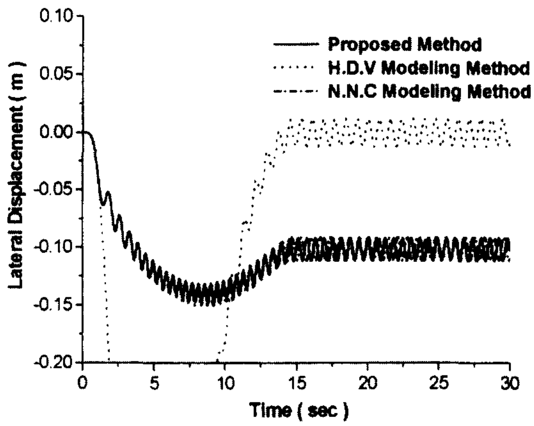

Fig. 5 Comparison of lateral displacement of simply supported beam at the middle point

of NNC modeling method. The accuracy of the results obtained by the NNC modeling method was verified in reference (Yoo, 1995).

4. Conclusions

A nonlinear modeling method is proposed for the dynamic analysis of flexible structures under going overall motion. Not only Cartesian deformation variables but also strain variables are employed in this modeling method. With the mixed variables all boundary conditions can be satisfied while geometric relations between strain variables and deformation variables are incorporated into the formulation. The reliability and the accuracy of the proposed modeling method are verified through the numerical study. It is found that accurate dynamic analysis results can be obtained with the proposed modeling method for two examples that have two distinct sets of boundary conditions.

Acknowledgment

This research was supported by Center of Innovative Design Optimization Technology (iDOT), Korea Science and Engineering Foundation.

References

Bodley, C., Devers, A. Park, A. and Frisch, H., 1978, "A digital Computer Program for the Dynamic Interaction Simulation of Controls and Structure (DISCOS)," *NASA TP-1219*, Vols. 1 & 2.

Christensen, E. and Lee, S., 1986, "Nonlinear Finite Element Modeling of the Dynamics of Unrestrained Flexible Structures," *Computers and Structures*, 23, pp. 819~829.

Frisch, H., 1975, "A Vector-Dyadic Development of the Equations of Motion for N-Coupled Flexible Bodies and Point Masses," *NASA TN D-8047*.

Goldstein, H., 1980, *Classical Mechanics*, Addison Wesley, Publishing Company.

Ho, J., 1977, "Direct Path Method for Flexible Multibody Spacecraft Dynamics," *Journal of Spacecraft and Rockets*, Vol. 14, pp. 102~110.

Hurty, W., Collins, J. and Hart, G., 1971, "Dynamic Analysis of Large Structures by Modal Synthesis Techniques," *Computers and Structures* 1, pp. 553~563.

Kane, T., Ryan, R. and Banerjee, A., 1987, "Dynamics of Cantilever Beam Attached to a Moving Base," *Journal of Guidance, Control and Dynamics*, 10, pp. 139~151.

Simo, J. and Vu-Quoc, L., 1986, "On the Dynamics of Flexible Beams Under Large Overall Motions-the Plane Case : Part I and Part II," *Journal of Applied Mechanics*, 53, pp. 849~863.

Southwell, R. and Gough, F., 1921, "The Free Transverse Vibration of Airscrew Blades," *British A. R. C. Reports and Memoranda* No. 766.

Yoo, H., 1992, "A Linear Dynamic Modeling Using Hybrid Deformation Variables for Rotating Structure," *Journal of The Korean Society for Aeronautical and Space Sciences*, Vol. 19, No. 3, pp. 32~39.

Yoo, H., 1995, "Dynamic Analysis of Simply Supported Flexible Structures Undergoing Large Overall Motion," Transaction of the KSME, Vol. 19, No. 6, pp. 1363~1370.